Journal of Hazardous Materials 182 (2010) 1–9

Contents lists available at ScienceDirect

Journal of Hazardous Materials

journal homepage: www.elsevier.com/locate/jhazmat

Preparation and utilization of wheat straw bearing amine groups for the sorption of acid and reactive dyes from aqueous solutions

Xing Xu, Bao-Yu Gao*, Qin-Yan Yue, Qian-Qian Zhong

School of Environmental Science and Engineering, Shandong University, Jinan 250100, PR China

ARTICLE INFO

Article history:
Received 21 September 2009
Received in revised form 14 March 2010
Accepted 15 March 2010
Available online 23 March 2010

Keywords:
Sorption
Equilibrium isotherm
Dyes
Kinetics
Modified wheat straw (MWS)
Thermodynamic

ABSTRACT

Removal of Acid Red 73 (AR 73) and Reactive Red 24 (RR 24) onto modified wheat straw (MWS) from aqueous solutions was investigated. Sorption experiments were carried out as function of MWS dosage, contact time, initial concentration, pH and temperature. Characterizations of MWS were measured and a mass of amine groups were observed in the framework of MWS. The equilibrium sorption data were well represented by the Langmuir isotherm equation, and the calculated thermodynamic parameters indicated a spontaneous and endothermic nature for sorption process. It was shown that pseudo-second-order kinetic equation could best describe the adsorption kinetics. More over, the high maximum sorption capacity ($q_{e\,max}$, 714.3 mg g^{-1} for AR 73 and 285.7 mg g^{-1} for RR 24) and low cost (1.24 US$ kg^{-1}) of MWS provided strong evidence of the potential of MWS for the technological applications of anionic dyes removal from aqueous solutions.

1. Introduction

Dyes are a kind of organic compounds which can bring bright and firm color to other substances. They have been widely used in the textile, leather, paper, rubber, plastics, cosmetics, pharmaceuticals and food industries. The presence of dyes in water, even at very low concentrations, will result in a considerable adverse aesthetic effect since they are visible pollutants. In addition, some dyes or their metabolites are either toxic or mutagenic and carcinogenic [1]. Many dyes are difficult to degrade, as they are generally stable to light, oxidizing agent and are resistant to aerobic digestion [2]. Hence, extensive use of dyes poses not only a severe public health concern, but also many serious environmental problems because of their persistence in nature and non-biodegradable characteristics.

The conventional methods of dye removal from industrial effluents include ion exchange, membrane technology, coagulation, oxidation or ozonation, flocculation and adsorption [3–6]. Amongst all, activated carbon is the most effective and commonly used sorbent for the treatment of dye wastewaters. However, its relatively high price, high operating costs and problems with regeneration of the spent carbon hamper its large scale application. This subsequently led to search for low cost, renewable, locally available materials as sorbent for the removal of dye colors.

A number of investigations have shown that some raw agricultural by-products have the potential of being used as alternative sorbent for the removal of dyes from wastewater, which include sawdust, rice hull [7], bagasse pith [8], barley husk [9], peanut hull [10], leaf [11] and other agricultural wastes [12,13]. Generally speaking, sorption capacity of raw agricultural by-products is very low. To improve the sorption capacity of crude agricultural by-products, various chemical modifications were employed [4,10,14]. An appropriate chemical composition in crude agricultural by-products with high contents of lignin, cellulose (as α-cellulose) and hemicelluloses [15,16], suggests a broad potential application to sorbent production; this is due to the large amount of easily available hydroxyl groups existing in the cellulose, hemicelluloses and lignin, which can easily make a series of chemical reactions, such as esterification, etherification and copolymerization [17,18].

Sorbent used in this work was prepared by the reaction of wheat straw (WS) with epichlorohydrin and trimethylamine in the presence of ethylenediamine and N,N-dimethylformamide [19]. Previous work in our laboratory has shown that modification of WS in this reaction yielded a material capable of removing both phosphate and nitrate [20,21]. In this paper, we reported the performance of modified wheat straw (MWS) as a sorbent for anionic Acid Red 73 (AR 73) and Reactive Red 24 (RR 24) sorption. The sorption capacities of MWS for AR 73 and RR 24 were investigated by determining the equilibrium isotherms. The effects of phase contact time, temperature and sorbent dosage on the dye adsorption were examined. In addition, kinetic studies were carried out taking the initial dye concentration into account.

* Corresponding author. Tel.: +86 531 88364832; fax: +86 531 88364513.
E-mail address: bygao@sdu.edu.cn (B.-Y. Gao).

0304-3894/$ – see front matter © 2010 Elsevier B.V. All rights reserved.
doi:10.1016/j.jhazmat.2010.03.071

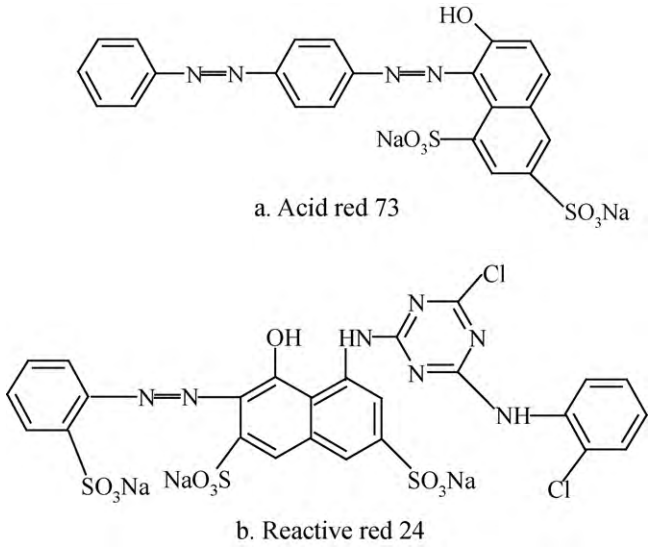

Fig. 1. Chemical structures of Acid Red 73 and Reactive Red 24.

2. Materials and methods

2.1. Sorbates: anionic dyes

The dyes used in this study are listed in Table 1. Their chemical structures are shown in Fig. 1. In aqueous solution, AR 73 and RR 24 were dissolved and the sulphonate groups of the dyes were dissociated and converted to anionic dye ions. The two dyes (AR 73 and RR 24), in commercial purity, were used without further purification. Concentrations of dye solutions prepared were calculated taking the dye content into consideration. Standard dye solutions of 1000 mg l^{-1} were prepared as stock solutions and subsequently diluted when necessary.

2.2. Sorbent: MWS

2.2.1. Preparation of MWS

WS was obtained from Liao Cheng, Shandong, China. The raw WS was washed with water, dried at 60 °C for 6 h and sieved into particles with diameters from 100 to 250 μm.

Ten grams of WS was reacted with 6 ml of epichlorohydrin and 5 ml of N,N-dimethylformamide in a 250 ml three-neck round bottom flask at 85 °C for 60 min. Two ml of ethylenediamine was added and the solution was stirred for 45 min at 8 °C, followed by adding 5 ml of 40% trimethylamine (w/w) and the mixture was stirred for 120 min at 85 °C. The product was washed with 500 ml of distilled water to remove the residual chemicals, dried at 60 °C for 12 h and sieved to obtain particles smaller than 250 μm in diameter and then used in all the sorption experiments (16.1 g of MWS was obtained).

The structure of MWS is demonstrated in Fig. 2.

Table 1
General characteristics of AR 73 and RR 24.

Name of dyes	AR 73	RR 24
Generic name	C.I. Acid Red 73	C.I Reactive Red 24
Chemical formula	$C_{22}H_{14}N_4Na_2O_7S_2$	$C_{25}H_{14}Cl_2N_7Na_3O_{10}S_3$
Molecular weight	556.490	808.482
CAS number	5413-75-2	–
λ_{max} (nm)	508	534
Appearance	Dark red	Red

2.2.2. Characterization of MWS

Specific surface area measurements were performed with an automatic BET surface area analyzer (Model F-Sorb 2400, Beijing Jinaipu Technical Apparatus Co., Ltd., China). The detection limit of this instrument, using N_2, is 0.01 m^2 g^{-1}.

The nitrogen content of MWS was measured by element analyzer (Elementar Vario EL III, Germany) to evaluate the grafted amine groups in the MWS.

Zeta potential measurements were carried out using a microelectrophoresis apparatus (JS94H, Shanghai Zhongchen Digital Technical Apparatus Co., Ltd., China) to determine the zeta potential of MWS and WS. To determine the zeta potential of MWS and WS at different pH values, the MWS and WS particles in the sediment phase were dispersed into the distilled water with pH range of 2.0–12.0.

The functional groups presenting in MWS and WS were investigated by using the FTIR technique (PerkinElmer "Spectrum BX" spectrometer). The spectrum was scanned from 400 to 4000 cm^{-1}.

Solid-state ^{13}C NMR spectra were acquired at room temperature on a Varian 400 Unity Inova spectrometer operating at 100.57 MHz and equipped with a 4 mm probe-head. All ^{13}C spectra were recorded under magic angle spinning (MAS) conditions at a spinning speed of 14 kHz. Improvements in the signal-to-noise ratio were gained by using cross-polarisation (CP) to transfer magnetization from proton to carbon. CP experiments were performed using a 2 s recycle delay and a 1000 μs contact time.

2.3. Dye sorption experiments

In the dosage studies, sorption measurements were conducted by mixing various amounts of MWS (0.01–0.4 g) with 50 ml of dye solutions (100 mg l^{-1}) in 100 ml Erlenmeyer flasks. Erlenmeyer flasks were shaken at 180 rpm in a thermostat. The Erlenmeyer flasks were placed for a short while, and then MWS and residual dye solutions were separated by 0.45 μm of microfiltration membrane. The residual concentration of each solution was determined

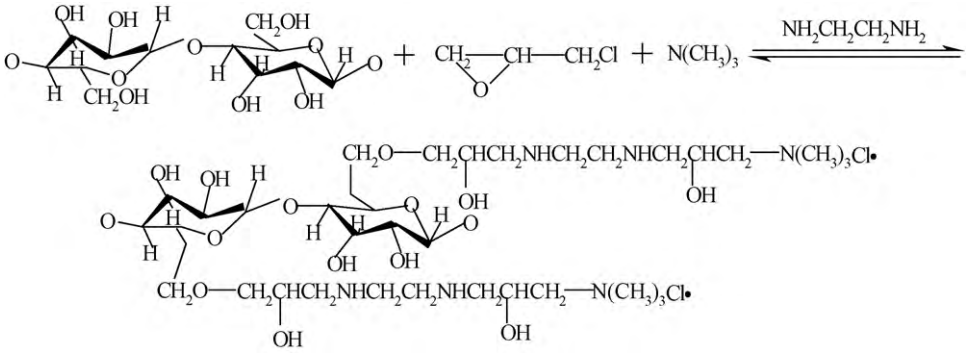

Fig. 2. Synthesis of MWS (cellulose as example).

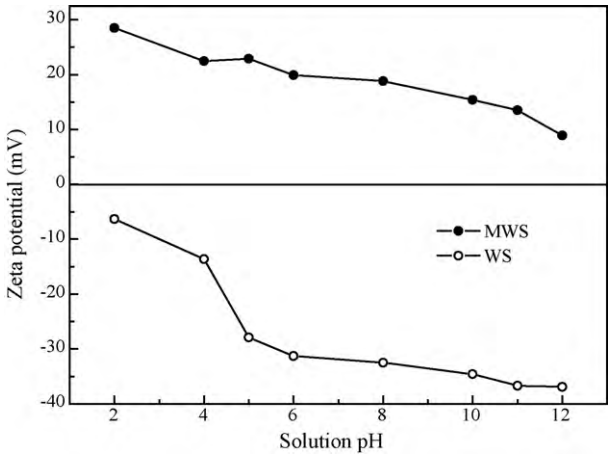

Fig. 3. Effect of pH on the zeta potential change of MWS and WS.

at the wavelengths of UV-maximum (λ_{max}) at 508 and 534 nm for AR 73 and RR 24, respectively, through the use of a UV–vis spectrophotometer (model UV754GD, Shanghai).

In the pH effect experiment, the initial solution pH (2.0–12.0) was first adjusted and then optimum amount of MWS (1 g l^{-1} for AR 73 and 1.6 g l^{-1} for RR 24) was added to several 100 ml Erlenmeyer flasks with 50 ml of 100 mg l^{-1} dye solutions. Then, equilibrium pH and dye concentrations in solutions were determined.

Sorption experiments were also carried out to obtain isotherms at different temperatures. This was done by maintaining the water bath with a magnetic stirrer at 20, 30, 40, 50 and 55 °C. In this group of experiments, 50 ml of dye solutions were used at 25–1000 mg l^{-1} concentrations for 540 min to allow attainment of equilibrium at constant temperatures. Sorption kinetic experiments were carried out at various concentrations of dye solutions (50, 80, 100 and 150 mg l^{-1}) using optimum amount of MWS at agitation speed of 180 rpm and 20 ± 1 °C. Samples of 1 ml were drawn from Erlenmeyer flasks at required time intervals and then were filtered to analyze for residual dye concentrations in solutions.

3. Results and discussion

3.1. Characterization of MWS

Specific surface area of MWS is about 8–12 m^2 g^{-1}, which is partially overlapped with the data of raw WS detected in the range of 6–15 m^2 g^{-1}; this result illustrates the fact that MWS do not have the similar porous structure in active carbon (specific surface area higher than 500 m^2 g^{-1}), indicating the absence of surface adsorption in the potential sorption mechanism.

Fig. 3 shows the zeta potential of MWS and WS at different pH values. Results shown in Fig. 3 indicate that the zeta potentials of WS keep negative in the range of pH values. In contrast with the WS, the zeta potential of MWS is positive in the designed pH range, which indicates the existence of positive-charge functional groups in the framework of MWS. However, a gradual decrease in zeta potential of MWS is observed with the increase in pH; this could be attributed to the pH-dependent functional groups existing in MWS, such as hydroxyl and carboxyl groups. These groups will exhibit a greater negative charge when the pH is increased, which results in the decrease in the positive charge of MWS. Similar result was reported in previous work of Meng [22].

Table 2 displays the elemental changes of carbon, hydrogen and nitrogen in MWS in comparison with WS. A slight increase is observed in the carbon contents (41.11–43.25%) and hydrogen contents (6.10–7.26%) of MWS, respectively. The significant increase

Table 2
Change of element content of WS.

	N %	C %	H %	References
WS	0.35	41.11	6.10	[20]
MWS	4.7	43.25	7.26	This study

in nitrogen content (0.4–4.7%) of MWS indicates that the reactions proceed efficiently and quite a number of amine groups have been introduced into the MWS. Similar result was observed in the previous work of Orlando for the preparation of agricultural residue anion exchangers, which have the nitrogen contents in the range of 4.5–5.0% [19].

Further analysis of MWS and WS was carried out using FTIR spectrophotometric studies (Fig. 4). The FTIR spectrum of MWS and WS exhibits a sharp adsorption band in the region of 3600–3400 cm^{-1}, which corresponds to the presence of free hydroxyl groups. The bands at 2920 and 1651 cm^{-1} indicate the presence of C–H aliphatic and aromatic in WS. The band at 607 cm^{-1} is associated with the special vibration of chloric alky groups. The intense vibration at 1337 cm^{-1} further validates the large number of grafted amine groups in the structure of MWS. Similar result was also reported in our previous work, with grafted amine groups observed at the band of 1350 cm^{-1} [20].

Fig. 5 shows the ^{13}C CP-MAS NMR spectra of WS and MWS. The spectra of WS are dominated by the set of resonances in the region between 60 and 120 ppm. In particular, the intense peak at 64 ppm is assigned to C-6 carbons of crystalline cellulose and 62 ppm to C-6 carbons of hemicelluloses (cellulose and hemicelluloses use the same monomer in Fig. 5). The shoulder at 84 ppm corresponds to C-4 carbons of crystalline cellulose and 82 ppm to C-4 of hemicelluloses. The resonance at 105 ppm is assigned to the anomeric carbon (C-1) of cellulose and the shoulder at 103 ppm to C-1 of hemicelluloses. The intense peaks at 73 and 75 ppm are overlapping signals due to the C-2, C-3, and C-5 carbons of all polysaccharides [23,24]. In Fig. 5(b), intense amine carbon peaks are present in the CP-MAS spectra of MWS (30–60 ppm) as compared to the spectra of WS, which is the result of the presence of the carbons of $–CH_2N–$ and $–NCH_3$, where the central chemical shifts for these peaks are located at 52 and 35 ppm, respectively [24]. Nevertheless, these signals are accounted together with the carbons of celluloses and hemicelluloses, which make it difficult to quantify each component.

Based on the characterization of MWS mentioned above, it is clear that the grafted functional groups in MWS would be beneficial to the sorption of anion dyes from solution.

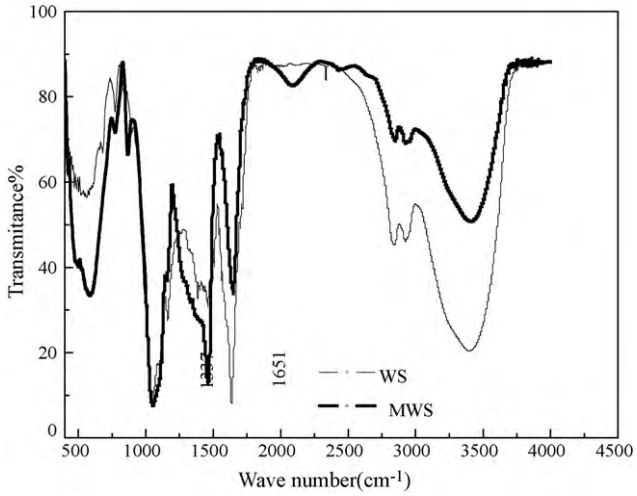

Fig. 4. FTIR analysis of MWS and WS.

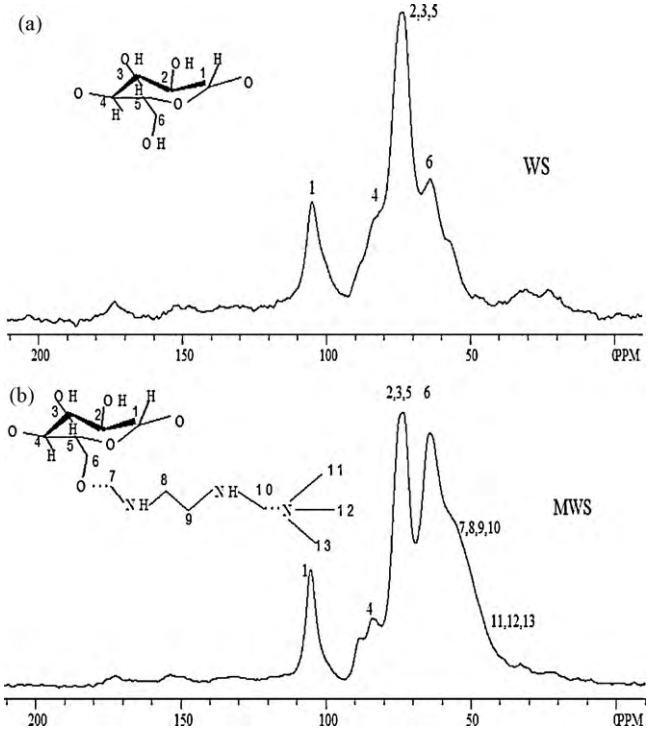

Fig. 5. ^{13}C CP-MAS NMR spectra of WS and MWS.

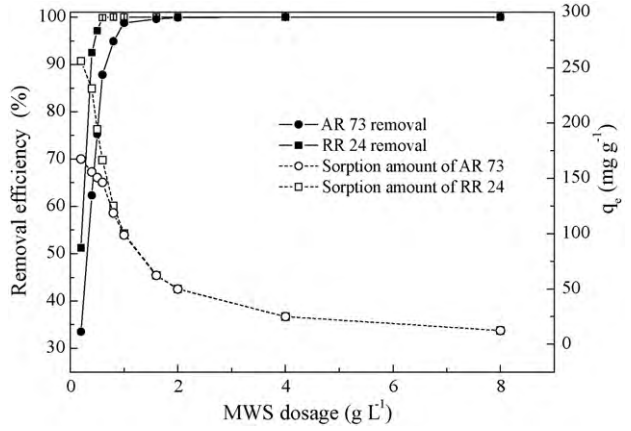

Fig. 6. Effect of MWS dosage on the sorption of AR 73 and RR 24 (initial dye concentration: 100 mg L^{-1}; temperature: 20 °C; shaker speed: 180 rpm; original solution pH 5.45 (RR 24), 6.32 (AR 73)).

3.2. Sorption properties of dyes

3.2.1. Effect of MWS dosage and contact time on the sorption process

The effect of MWS dosage on the sorption of AR 73 and RR 24 was studied by varying the concentration of the sorbent from 0.2 to 8 g l^{-1} while keeping the other experimental conditions constant. The percentage removal of AR 73 and RR 24 versus MWS dosage is shown in Fig. 6. An increase in the percentage of sorption with increasing MWS dosage is observed in both two dyes. This is due to the availability of more surface functional groups at higher MWS dosage. Along with the increase of sorbent dosage from 0.2 to 0.6 g l^{-1} the percentages of dye sorbed increase from 30.41 to 99.9% and from 34.49 to 89.5% in AR 73 and RR 24, respectively; this suggests that MWS is more effective for AR 73 removal than RR 24. As indicated in Fig. 6, the amount of dye adsorbed per unit weight of the sorbent (q_e) decreases with increase in dosage. When the dyes removal reaches to near 100%, additional MWS added would not be used, and the q_e would become lower because the capacity is normalized by added MWS.

For both the sorption processes, sorption experiments were carried out for different contact times with sorbent dose selected as 0.6, 1, 1.6 and 2 g l^{-1} (Fig. 7). Results shown in Figs. 6 and 7 indicate that equilibrium occurs at 0.6 and 1 g l^{-1} of MWS dosage for AR 73 and RR 24, respectively. However, a significant increase of equilibrium time for AR 73 (180 min) and RR 24 (120 min) sorption is observed in this dosage conditions, compared with the equilibrium time for AR 73 (45 min) and RR 24 (30 min) when MWS dosages are selected at 1 and 1.6 g l^{-1}, respectively. Based on the consideration for shortening sorption equilibrium time, 1 g l^{-1} for AR 73 and 1.6 g l^{-1} for RR 24 are fixed as optimum MWS dosages and used in subsequent experiment.

3.2.2. Effect of pH on the sorption process

Fig. 8 shows the effect of initial solution pH on the adsorptive removal of AR 73 and RR 24 by MWS. The results show that when initial solution pH is increased from 2.5 to 12.0, the percentage removal of AR 73 and RR 24 on the MWS keeps almost constant with the increase of pH from 2.5 to 8.0 and then decreases with the pH from 8.0 to 12.0. An examination of the solution pH values indicates that the equilibrium solution pH values after the sorption experiments decrease significantly in comparison with the initial solution pH values (Fig. 8). When the initial solution pH is in the range of 2.5–8.0, equilibrium solution pH values are below 5.0 and the dyes removal efficiency are almost 100% in this condition. As the initial solution pH increases from 8.0 to 12.0, equilibrium solution pH values dramatically increase from 5.0 to 11.0 and the dyes removal efficiency gradually decrease from 99% to 85%. As shown in some literature, the removal efficiency of some anionic adsorbates on the sorbents with positive surface charges often displayed a general trend of decrease with the increase of solution pH values, attributed to abundant of OH^- and the less attractive or more repulsive electrostatic interaction at higher solution pH values [25,26].

It seems likely that sorption mechanism of AR 73 and RR 24 onto MWS may be as follows: first AR 73 and RR 24 were dissolved in an aqueous solution after which the sulphonate groups of AR 73 and RR 24 (R–SO_3Na) became dissociated and converted to anionic dye ions. The sorption process then proceeded due to the interaction between the anionic dye ions and the functional groups of MWS (R–N^+ (CH_2CH_3)$_3Cl^-$) formulated as follows [27,28]:

$$R\text{–}SO_3Na \xrightarrow{H_2O} R\text{–}SO_3^- + Na^+ \quad (1)$$

$$R'\text{–}N^+(CH_2CH_3)_3Cl^- + Na^+{}^-O_3S\text{–}R \rightleftharpoons R'\text{–}N(CH_2CH_3)_3{}^+{}^-O_3S\text{–}R + NaCl \quad (2)$$

As the pH values increase, the amine groups (R–N (CH_2CH_3)$_3^+$) for dyes sorption will decrease on the outer surface of the sorbent due to the presence of excess OH^- ions competing with dye anions (R–SO_3^-) for sorption sites and a result of the sorption decreases [29].

Based on the mentioned consideration, all further studies can be carried out at initial pH in the range of 2.5–8.0 for both AR 73 and RR 24.

3.2.3. Effect of temperature

Temperature is an important parameter for the sorption process. Fig. 9 illustrates the effect of temperature (20, 30, 40, 50 and 55 °C) on the sorption of AR 73 and RR 24 by MWS. The results reveal that the dyes uptake increases with increasing temperature from 20 to 55 °C. The fact that the sorption of dyes is in favour of temperature indicates that the increase in temperature would increase the

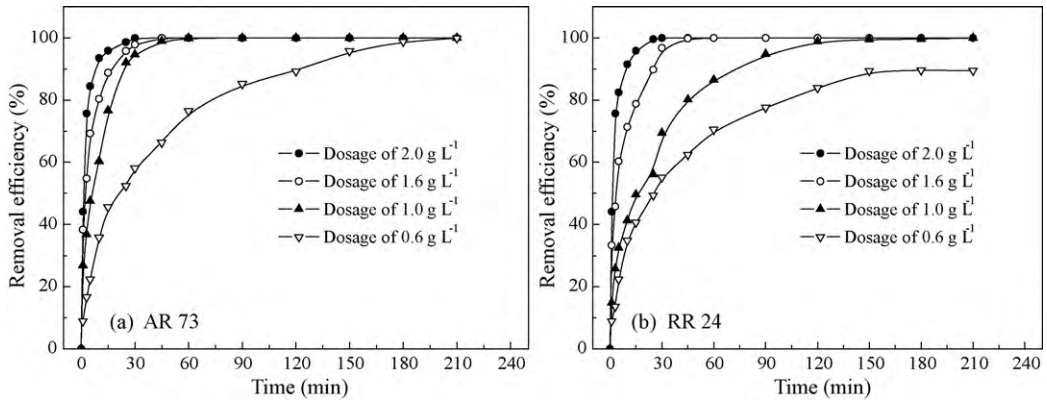

Fig. 7. Effect of contact time on the sorption process (initial dye concentration: 100 mg L^{-1}; temperature: 20 °C; shaker speed: 180 rpm; original solution pH 5.45 (RR 24), 6.32 (AR 73)).

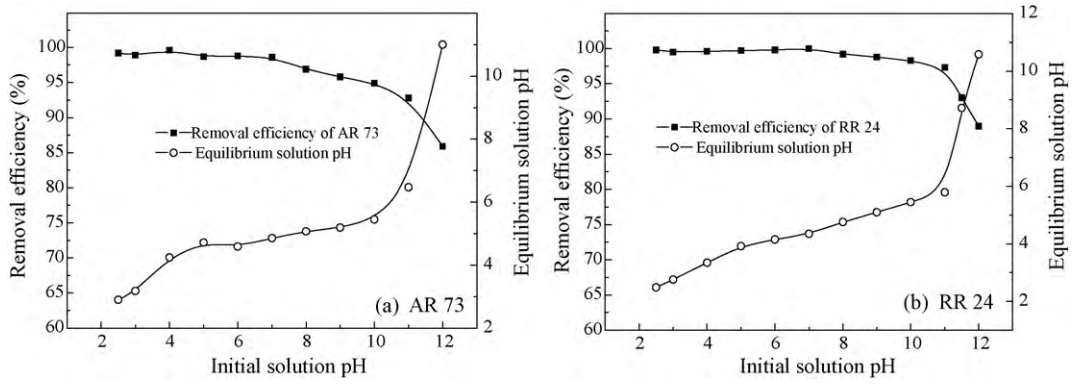

Fig. 8. Effect of initial pH on the sorption process (initial dye concentration: 100 mg L^{-1}; temperature: 20 °C; shaker speed: 180 rpm; MWS dosages: 1 g L^{-1} for AR 73 and 1.6 g L^{-1} for RR 24).

mobility of the large dye ions as well as produce a swelling effect with in the internal structure of the MWS, thus enabling the large dye molecules to penetrate further [30]. Therefore, the enhancement in sorption with the temperature may largely depend on the increase in interaction between the functional groups on the sorbent surface sites and the adsorbate. This may be also a result of the decrease in the thickness of the boundary layer surrounding the sorbent with the temperature, so that the mass transfer resistance of adsorbate in the boundary layer decreases [31].

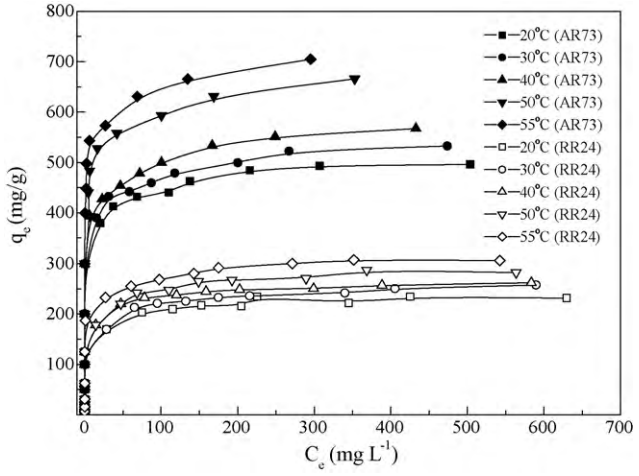

Fig. 9. Sorption isotherms for AR 73 and RR 24 onto MWS at different temperatures (MWS dosages: 1 g L^{-1} for AR 73 and 1.6 g L^{-1} for RR 24; shaker speed: 180 rpm).

3.2.4. Sorption isotherms

The sorption results were analyzed to see whether the isotherm obeyed the Langmuir, Freundlich and Dubinin–Radushkevich (D–R) isotherm models equations [30–32].

Langmuir equation:

$$\frac{1}{q_e} = \frac{1}{q_{max}} + \left(\frac{1}{q_{max} K_L}\right) \frac{1}{C_e} \quad (3)$$

Freundlich equation:

$$\ln\ q_e = \ln K_F + \frac{1}{n} \ln C_e \quad (4)$$

D–R eq:

$$\ln q_e = \ln q_m - \beta\varepsilon^2 \quad (5)$$

where C_e the equilibrium dye concentration in solution (mg l^{-1}); q_{max}, the monolayer capacity of the sorbent (mg g^{-1}); K_L, the Langmuir constant (l mol^{-1}); K_F, the Freundlich constant (l g^{-1}); β, a constant related to the mean free energy of adsorption per mole of the adsorbate (mol^2 kJ^{-2}); ε, the Polanyi potential, which is equal to $RT \ln(1 + (1/Ce))$ and q_m, the theoretical saturation capacity, which is used only in maximum sorption process.

The Langmuir, Freundlich and D–R parameters for the sorption of AR 73 and RR 24 onto MWS are listed in Table 3. The fit of the data suggests that the Langmuir model gives slightly closer fittings than those of Freundlich and D–R models. The q_e calculated from Langmuir model (Table 3) increase with increasing temperature, which indicates that the sorption process for the two dyes is an endothermic reaction.

The essential feature of the Langmuir isotherm can be expressed by means of a dimensionless constant separation factor or equilib-

Table 3
Isotherm constants for sorption of RA 73 and RR 24.

T°C	RA 73					RR 24				
	Equation	q_{max} (mg g^{-1})	K_L (L mg^{-1})	R_L	R^2	Equation	q_{max} (mg g^{-1})	K_L	R_L	R^2
Langmuir model										
20	$C_e/q_e = 0.002C_e + 0.018$	500	0.111	<0.31	0.999	$C_e/q_e = 0.0043C_e + 0.023$	232.6	0.187	<0.18	0.999
30	$C_e/q_e = 0.00182C_e + 0.015$	549.1	0.121	<0.25	0.998	$C_e/q_e = 0.0040C_e + 0.020$	250.0	0.200	<0.17	0.998
40	$C_e/q_e = 0.0018C_e + 0.011$	555.6	0.164	<0.21	0.999	$C_e/q_e = 0.0039C_e + 0.019$	256.4	0.205	<0.17	0.999
50	$C_e/q_e = 0.00146C_e + 0.008$	678.9	0.186	<0.12	0.998	$C_e/q_e = 0.0037C_e + 0.018$	270.2	0.207	<0.16	0.999
55	$C_e/q_e = 0.0014C_e + 0.003$	714.3	0.467	<0.08	0.998	$C_e/q_e = 0.0035C_e + 0.016$	285.7	0.217	<0.18	0.998
T°C	Equation	K_F (L g^{-1})	n	R^2		Equation	K_F (L g^{-1})	n	R^2	
Freundlich model										
20	$\ln q_e = 0.102 \ln C_e + 5.63$	273.9	9.80	0.967		$\ln q_e = 0.0785 \ln C_e + 4.96$	142.5	12.73	0.955	
30	$\ln q_e = 0.100 \ln C_e + 5.52$	246.7	10	0.951		$\ln q_e = 0.082 \ln C_e + 5.03$	152.4	12.16	0.954	
40	$\ln q_e = 0.105 \ln C_e + 5.73$	307.8	9.52	0.922		$\ln q_e = 0.093 \ln C_e + 5.01$	149.8	10.75	0.968	
50	$\ln q_e = 0.097 \ln C_e + 5.86$	359.6	10.3	0.931		$\ln q_e = 0.0902 \ln C_e + 5.23$	191.4	11.1	0.938	
55	$\ln q_e = 0.098 \ln C_e + 5.04$	154.4	10.2	0.936		$\ln q_e = 0.0898 \ln C_e + 5.11$	165.6	11.14	0.946	
T°C	Equation	q_{max} (mg g^{-1})	β	E_a (kJ mol^{-1})	R^2	Equation	q_{max} (mg g^{-1})	B	E_a (kJ mol^{-1})	R^2
D–R model										
20	$\ln q_e = -0.0009\varepsilon^2 - 6.79$	628.2	0.0009	23.8	0.982	$\ln q_e = -0.0015\varepsilon^2 - 7.89$	292.2	0.0015	18.3	0.972
30	$\ln q_e = -0.0008\varepsilon^2 - 6.76$	632.5	0.0008	27.8	0.969	$\ln q_e = -0.0012\varepsilon^2 - 7.78$	314.6	0.0012	24.9	0.980
40	$\ln q_e = -0.0005\varepsilon^2 - 6.75$	651.5	0.0005	32.2	0.975	$\ln q_e = -0.0008\varepsilon^2 - 7.82$	311.5	0.0008	25.0	0.97
50	$\ln q_e = -0.0009\varepsilon^2 - 6.58$	756.8	0.0009	23.8	0.971	$\ln q_e = -0.0007\varepsilon^2 - 7.76$	332.9	0.0007	27.9	0.978
55	$\ln q_e = -0.0006\varepsilon^2 - 6.47$	861.9	0.0006	28.9	0.963	$\ln q_e = -0.0008\varepsilon^2 - 7.74$	352.8	0.0008	25.0	0.964

rium parameter R_L, which is calculated using the following equation [32].

$$R_L = \frac{1}{1 + K_L C_0} \quad (6)$$

where C_0 is initial concentration (mg l^{-1}). The values of R_L calculated as above equation are incorporated in Table 3. All the R_L values are in the range of 0–1, which confirms the favorable uptake of AR 73 and RR 24.

The constant β in D–R model gives an idea about the mean free energy E (kJ mol^{-1}) of sorption per molecule of the adsorbate when it is transferred to the surface of the solid from infinity in the solution and can be calculated using the relationship [33].

$$E = \frac{1}{(2\beta)^2} \quad (7)$$

The magnitude of E for AR 73 and RR 24 sorption are in the range of 23.8–32.2 and 18.3-25.0 kJ mol^{-1}, respectively. This range of mean free energies is typical for ion exchange, which indicates that anion exchange is the main sorption mechanism for the sorption process [34].

3.2.5. Thermodynamic parameters

Thermodynamic parameters provide in-depth information of inherent energetic changes associated with sorption; the thermodynamic parameters such as change in standard free energy ΔG^0, enthalpy (ΔH^0) and entropy ΔS^0 were calculated to elucidate the process of sorption. The Langmuir isotherm was applied to calculate the thermodynamic parameters via Eqs. (8) and (9) [35,36]:

$$\Delta G^0 = -RT \ln(K_L) \quad (8)$$

$$\ln(K_L) = \frac{\Delta S^0}{R} - \frac{\Delta H^0}{RT} \quad (9)$$

where K_L is Langmuir equilibrium constant (L mol^{-1}), R is the universal gas constant, 8.314 J mol^{-1} K, T is the absolute temperature. The enthalpy change was determined by plotting $\ln K_L$ versus $1/T$.

The thermodynamic parameters are listed in Table 4. The negative values of ΔG^0 indicate that the sorption of the anionic dyes onto MWS is spontaneous and thermodynamically favorable. The increase in the value of $-\Delta G^0$ with increasing temperature indicates that the sorption process is more favorable at higher temperature. A positive ΔH^0 suggests that the sorption of AR 73 and RR 24 onto MWS is endothermic, which is supported by the increasing sorption of these dyes with the increase in temperature. In addition, the positive value of ΔS^0 suggests a increase in degree of freedom at the solid–liquid interface during sorption process, which reflects increased randomness at the solid/solution interface and dyes affinity to MWS. Similar results were observed for sorption of Acid Red 57 on surfactant-modified sepiolite [25].

3.2.6. Sorption kinetics

Sorption kinetics, demonstrating the solute uptake rate, is one of the most important characteristics which represents essential information on the reaction pathways, and therefore, determines their potential applications.

Sorption of AR 73 and RR 24 onto MWS at different initial dye concentrations are shown in Fig. 10. The AR 73 sorption rates increase dramatically in the first 20 min for various initial concentrations, and reach equilibrium gradually at 25, 30, 45 and 60 min, corresponding to AR 73 initial concentrations of 50, 80, 100 and 150 mg l^{-1}, respectively. Similar result is also observed in the sorption of RR 24. To analyze the sorption rate of AR 73 and RR 24 onto MWS, the pseudo-first-order equation, pseudo-second-order equation and intra-particle diffusion equation were evaluated based on the experimental data.

Table 4
Thermodynamic parameters for adsorption of phosphate onto WR-AE.

Dyes	T (K)	ΔG^0 (kJ mol^{-1})	ΔH^0 (kJ mol^{-1})	ΔS^0 (J/mol K)
AR 73	293	−26.87	32.4	214.6
	303	−27.88		
	313	−29.72		
	323	−32.56		
	328	−34.0		
RR 24	293	−29.05	4.53	135.1
	303	−30.67		
	313	−31.27		
	323	−32.39		
	328	−32.93		

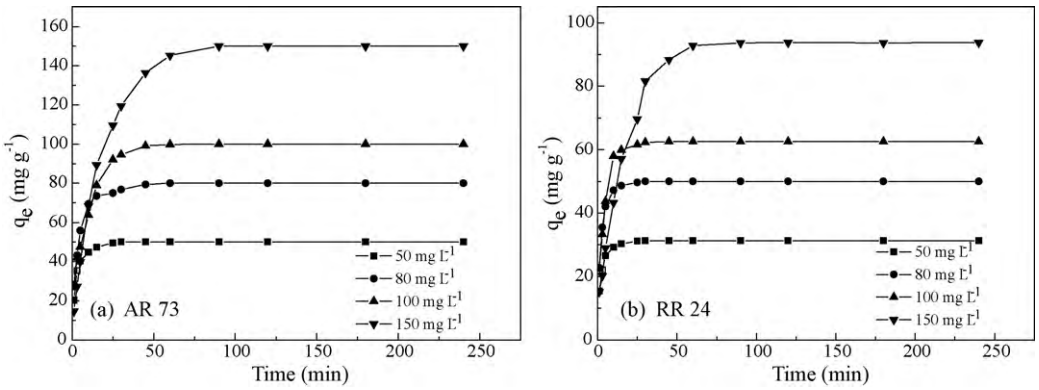

Fig. 10. Sorption of AR 73 and RR 24 onto MWS at different initial dye concentrations (temperature: 20 °C; MWS dosages: 1 g L^{-1} for AR 73 and 1.6 g L^{-1} for RR 24; shaker speed: 180 rpm).

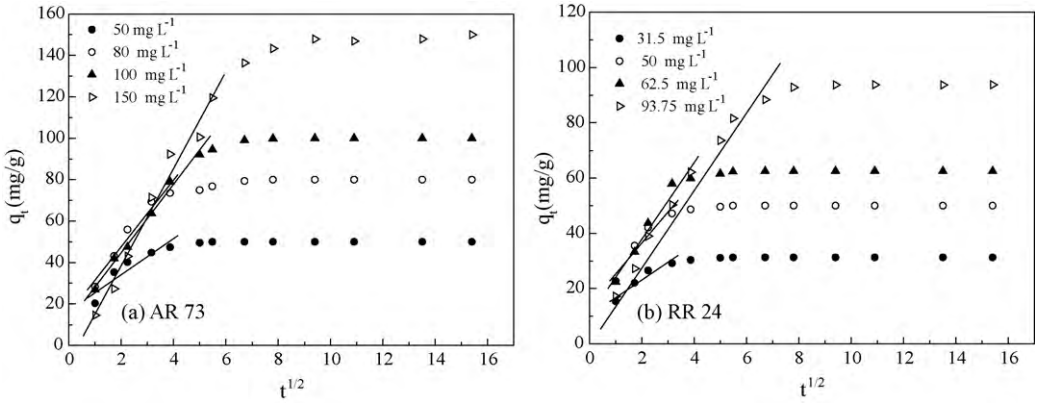

Fig. 11. Intra-particle diffusion kinetics for sorption of AR 73 and RR 24 dye s onto MWS at 20 °C.

(1) Pseudo-first-order model

A kinetic model for adsorption analysis is the pseudo-first-order rate expressed in the form [20]:

$$\ln(q_e - q_t) = \ln\ q_e - k_1 t \tag{10}$$

where q_e and q_t are the amounts of dyes sorbed per gram MWS at equilibrium and time t (mg g^{-1}), respectively; k_1 is the rate constant of pseudo-first-order (min^{-1}).

(2) Pseudo-second-order model

The pseudo-second-order kinetic rate equation is given as follows [28]:

$$\frac{t}{q_t} = \frac{1}{k_2 q_e^2} + \frac{t}{q_e} \tag{11}$$

where k_2 is the equilibrium rate constant of pseudo-second-order (g (mg min)$^{-1}$).

(3) Intra-particle diffusion model

The two models above can not identify the diffusion mechanism, so the intra-particle diffusion model was proposed. The initial rate of intra-particle equation is the following [37,38]:

$$q_t = k_p t^{0.5} \tag{12}$$

where k_p is the intra-particle rate constant (g mg^{-1} $min^{-0.5}$), and the intra-particle rate constant k_p is a function of equilibrium concentration in solid phase q_e and intra-particle diffusivity D according to the equation expressed as

$$k_p = \frac{6q_e}{R}\sqrt{\frac{D}{\pi}} \tag{13}$$

where R is the particle radius and D is intra-particle diffusivity.

Table 5
Kinetic parameters for adsorption rate expressions.

Dye	C_0 (mg l^{-1})	$q_{e\,exp}$ [a] (mg g^{-1})	Pseudo-first-order			Pseudo-second-order			Intra-particle diffusion	
			k_1 (min^{-1})	q_{e1} [b] (mg g^{-1})	R^2	k_2 (g (mg min) $^{-1}$)	q_{e2} [b] (mg g^{-1})	R^2	k_p (mg (g min)$^{-1}$)	R^2
AR 73	150	149.9	0.055	146.7	0.995	0.00066	152.3	0.9991	22.0	0.978
	100	99.9	0.099	89.9	0.995	0.003	102.0	0.9996	15.4	0.987
	80	80.0	0.092	40.3	0.958	0.0079	80.6	0.9999	16.1	0.959
	50	50.0	0.162	27.0	0.988	0.025	50.3	1	4.22	0.923
RR 24	150	93.75	0.062	85.6	0.987	0.0013	95.2	0.9992	15.1	0.991
	100	62.5	0.173	47.2	0.972	0.014	62.9	0.9999	13.8	0.960
	80	50	0.177	22.9	0.971	0.034	50.3	0.9999	11.2	0.928
	50	31.25	0.194	16.4	0.992	0.052	31.3	1	6.42	0.930

[a] $q_{e,exp}$ is experimental values.
[b] q_{e1}, q_{e2} are calculated values.

Table 6
Comparison of the q_e of some dyes on various sorbents.

Dyes	Sorbents	$q_{e\,max}$ (mg g^{-1})	Reference
AR 73	MWS	714.3	This work
RR 24	MWS	285.7	This work
AR 73	$[CuBDP]_n$ solid waste	364	[39]
RR 24	Sludge activated carbon	35.7	[40]
AR 73	Seed shells	204	[41]
RR 24	Chitosan	245	[42]
AR 73	Activated carbon	43	[43]
RR 24	Activated carbon	23	[43]

Table 7
Chemical costs in RMB/kg.

Chemical	Price RMB (kg^{-1})
Epichlorohydrin	8.5
DMF	5.8
Raw WS	No cost
Ethylenediamine	13.3
Triethylamine	10.2
Distilled water	0.05
Stills cost (electricity and heat cost): 0.4 RMB for 1 kg of MWS	

The kinetic parameters under different conditions were calculated and are given in Table 5. The correlation coefficients (R^2), for the pseudo-first-order kinetic model are between 0.971 and 0.995 and the correlation coefficients (R^2), for the pseudo-second-order kinetic model are 0.999 (figures are omitted). And also, the calculated q_{e2} values agree well with experimental $q_{e,exp}$ values. It is probable, therefore, that this sorption system is not a first-order reaction, it fits the pseudo-second order. Similar results were reported for the sorption of basic red 22 onto pith [36].

If the plot of uptake, qt, versus square root of time, $t^{1/2}$ passes through the origin, the intra-particle diffusion will be the sole rate-limiting process [38]. In the study, the plots of qt versus $t^{1/2}$ exhibit an initial linear portion followed by a plateau which occurs after 30–60 min (Fig. 11). The initial curved portion of the plots seems to be due to boundary layer sorption and the linear portion to intra-particle diffusion, with the plateau corresponding to equilibrium. However, the plots do not pass through the origin. This indicates that although intra-particle diffusion is involved in the sorption process, it is not the only rate-limiting step; other kinetic processes are simultaneously occurring and contribute to the sorption mechanism [38].

3.2.7. Evaluation of MWS

Table 6 shows the comparison of the maximum sorption capacities $q_{e\,max}$ of various sorbents for dyes. The values of $q_{e\,max}$ in this study (714.3 mg g^{-1} for AR 73 and 285.7 mg g^{-1} for RR 24) are larger than those in most of previous studies. This indicates that anionic dyes can be readily sorbed by MWS used in this study.

The agricultural waste, WS, used in this study can be easily obtained in China with low cost and simply modified for application. The cost of producing MWS was estimated assuming chemical costs for laboratory use and stills cost. The currents market prices in China of the chemicals utilized are shown in Table 7.

Assuming that 1.61 g of MWS can be produced from 1 kg of WS, the chemical cost and stills cost based on the proportions used in laboratory is approximately 8.96 RMB kg^{-1} (1.29 US$ kg^{-1}) of MWS, which is much lower than the AR-AE (5.3 US$ kg^{-1}) prepared in Orlando's studies [19].

4. Conclusions

This study investigated the equilibrium and kinetics of the sorption of anionic dyes onto MWS. The highest dye removal results could be achieved at initial pH in the range of 2.5–8.0. The sorption of AR 73 and RR 24 onto MWS was endothermic in nature with the dye removal capacity increasing with increasing temperature due to the increasing mobility of the large dye ions and the swelling effect with in the internal structure of the MWS.

The fit of the data suggested that the Langmuir model gave slightly closer fittings than those of Freundlich and D–R models. The R_L values showed that MWS was favorable for the sorption of AR 73 and RR 24. The negative values of standard free energy (ΔG^0) and enthalpy (ΔH^0) indicated that the sorption was a spontaneous and exothermic process. Pseudo-second-order equation generated the best agreement with experimental data for adsorption systems, and intra-particle diffusion was involved in the sorption process, it was not the only rate-limiting step. Results of batch sorption tests showed that MWS was efficient, low cost and alternative used as a sorbent for anionic dyes in aqueous solutions.

Acknowledgments

The research was supported by the National Natural Science Foundation of China (50878121), the Key Projects in the National Science & Technology Pillar Program in the Eleventh Five-year Plan Period (No. 2006BAJ08B05), the Science and Technology Development Key Program of Shandong Province, China (No. 2006GG2206007).

References

[1] S. Wang, Y. Boyjoo, A. Choueib, H. Zhu, Removal of dyes from solution using fly ash and red mud, Water Res. 39 (2005) 129–138.
[2] Y.C. Wong, Y.S. Szeto, W.H. Cheung, G. McKay, Equilibrium studies for acid dye adsorption onto chitosan, Langmuir 19 (2003) 7888–7894.
[3] S. Chinwetkitvanich, M. Tuntoolvest, T. Panswad, Anaerobic decolorization of reactive dyebath effluents by a two-stage UASB system with tapioca as a co-substrate, Water Res. 34 (2000) 222–232.
[4] G. Petzold, S. Schwarz, M. Mende, W. Jaeger, Dye flocculation using polyampholytes and polyelectrolyte-surfactant nanoparticles, J. Appl. Polym. Sci. 104 (2007) 1342–1349.
[5] M. Gholam, S. Nasseri, M.R. Alizadehfard, A. Mesdaghinia, Textile dye removal by membrane technology and biological oxidation, Water Qual. Res. J. Canada 38 (2003) 379–391.
[6] A. Lopez, H. Benbelkacem, J.S. Pic, H. Debellefontaine, Oxidation pathways for ozonation of azo dyes in a semi-batch reactor: a kinetic parameters approach, Environ. Technol. 25 (2004) 311–321.
[7] Y. Guo, J. Zhao, H. Zhang, S. Yang, J. Qi, Z. Wang, Use of rice husk based porous carbon for adsorption of rhodamine B from aqueous solutions, Dyes Pigments 66 (2005) 123.
[8] I.D. Mall, V.C. Srivastava, N.K. Agarwal, Removal of Orange-G and methyl violet dyes by adsorption onto bagasse fly ash-kinetic study and equilibrium isotherm analyses, Dyes Pigments 69 (2006) 210–223.
[9] T. Robinson, B. Chandran, P. Nigam, Effect of pretreatments of three waste residues, wheat straw, corncobs and barley husks on dye adsorption, Bioresour. Technol. 85 (2002) 119–124.
[10] R.M. Gong, Y. Ding, M. Li, C. Yang, H.J. Liu, Y.Z. Sun, Utilization of powdered peanut hull as biosorbent for removal of anionic dyes from aqueous solution, Dyes Pigments 64 (2005) 187–192.
[11] K.G. Bhattacharyya, A. Sarma, Adsorption characteristics of the dye, brilliant green, on neem leaf powder, Dyes Pigments 57 (2003) 211–222.
[12] R.M Gong, M. Li, C. Yang, Y.Z. Sun, J. Chen, Removal of cationic dyes from aqueous solution by adsorption on peanut hull, J. Hazard. Mater. 121 (2005) 247–250.
[13] T. Robinson, P. Chandran, P. Nigam, Removal of dyes from a synthetic textile dye effluent by biosorption on apple pomace and wheat straw, Water Res. 36 (2002) 2824–2830.
[14] T. Girek, C.A. Kozlowski, J.J. Koziol, W. Walkowiak, I. Korus, Polymerisation of beta-cyclodextrin with succinic anhydride. Synthesis, characterization, and ion flotation of transition metals, Carbohydr. Polym. 59 (2005) 211–215.
[15] R.M. Gong, Y.B. Jin, J. Chen, Y. Hu, J. Sun, Removal of basic dyes from aqueous solution by sorption on phosphoric acid modified rice straw, Dyes Pigments 73 (2007) 332–335.
[16] V. Piero, V. Gianpietro, Analysis of energy comparison for crops in European agricultural systems, Biomass Bioenergy 25 (2007) 235–255.
[17] O.E. Yilmaz, A. Sirit, M. Yilmaz, A calyx[4] arene oligomer and two beta-cyclodextrin polymers: synthesis and sorption studies of azo dyes, J. macromol. Sci. Pure 44 (2007) 167–173.
[18] M.A. Gaffar, S.M. El-Rafie, K.F. El-Tahlawy, Preparation and utilization of ionic exchange resin via graft copolymerization of beta-CD itaconate with chitosan, Carbohydr. Polym. 56 (2004) 387–396.

[19] U.S. Orlando, A.U. Baes, W. Nishijima, Preparation of agricultural residue anion exchangers and its nitrate maximum exchange capacity, Chemosphere 48 (2002) 1041–1046.
[20] X. Xu, B.Y. Gao, W.Y. Wang, Q.Y. Yue, Y. Wang, S.Q. Ni, Adsorption of phosphate from aqueous solutions onto modified wheat residue: characteristics, kinetic and column studies, Colloids Surf. B 70 (2009) 46–52.
[21] Y. Wang, B.Y. Gao, W.W. Yue, Q.Y. Yue, Adsorption kinetics of nitrate from aqueous solutions onto modified wheat residue, Colloids Surf. A 308 (2007) 1–5.
[22] I.H. Yoon, X.G. Meng, C. Wang, K.W. Kim, S. Bang, E. Choe, L. Lippincott, Perchlorate adsorption and desorption on activated carbon and anion exchange resin, J. Hazard. Mater. 164 (2009) 87–94.
[23] V. Singh, A.K. Sharma, D.N. Tripathi, R. Sanghi, Poly(methylmethacrylate) grafted chitosan: an efficient adsorbent for anionic azo dyes, J. Hazard. Mater. 161 (2009) 955–966.
[24] A. Baraka, P.J. Hall, M.J. Heslop, Preparation and characterization of melamine formaldehyde–DTPA chelating resin and its use as an adsorbent for heavy metals removal from wastewater, React. Funct. Polym. 67 (2007) 585–600.
[25] A. Ozcan, A.S. Ozcan, Adsorption of acid red 57 from aqueous solutions onto surfactant-modified sepiolite, J. Hazard. Mater. 125 (2005) 252–259.
[26] P.K. Malik, Use of activated carbons prepared from sawdust and rice-husk for adsorption of acid dyes: a case study of Acid Yellow 36, Dyes Pigments 56 (2003) 239–249.
[27] G. Annaduraia, L.Y. Ling, J.F. Lee, Adsorption of reactive dye from an aqueous solution by chitosan: isotherm, kinetic and thermodynamic analysis, J. Hazard. Mater. 152 (2008) 337–346.
[28] M. Wawrzkiewicz, Z. Hubicki, Kinetic studies of dyes sorption from aqueous solutions onto the strongly basic anion-exchanger Lewatit MonoPlus M-600, Chem. Eng. J. 150 (2009) 509–515.
[29] Z. Wu, I.S. Ahn, C.H. Lee, J.H. Kim, Y.G. Shul, K. Lee, Enhancing the organic dye adsorption on porous xerogels, Colloids Surf. A 240 (2004) 157–164.
[30] S.M. Venkat, D.M. Indra, C.S. Vimal, Use of bagasse fly ash as an adsorbent for the removal of brilliant green dye from aqueous solution, Dyes Pigments 73 (2007) 269–278.
[31] M. Wawrzkiewicz, Z. Hubicki, Equilibrium and kinetic studies on the adsorption of acidic dye by the gel anion exchanger, J. Hazard. Mater. 172 (2009) 868–874.
[32] K.R. Hall, L.C. Eagleton, A. Acrivos, T. Vermeulen, Pore and solid diffusion kinetics in fixed-bed adsorption under constant pattern conditions, Ind. Eng. Chem. Res. Fundam. 5 (1966) 212–223.
[33] S.M. Hasany, M.H. Chaudhary, Sorption potential of Hare river sand for the removal of antimony from acidic aqueous solution, Appl. Radiat. Isotopes 47 (1996) 467–471.
[34] M. Jain, V.K. Gar, K. Kadirvelu, Adsorption of hexavalent chromium from aqueous medium onto carbonaceous adsorbents prepared from waste biomass, J. Environ. Manage 91 (2010) 949–957.
[35] M. Ajmal, A.H. Khan, S. Ahmad, A. Ahmad, Role of sawdust in the removal of copper (II) from industrial wastes, Water Res. 32 (1998) 3085–3091.
[36] J.R. Huang, W.C. Hu, H.I. Chen, W.C. Liu, Comparative study of hydrogen sensing characteristics of a Pd/GaN Schottky diode in air and N_2 atmospheres, Sens. Actuators B: Chem. 123 (2007) 1040–1048.
[37] W.J. Weber, J. Morris, Kinetics of adsorption on carbon from solution, J. Sanitary Eng. Div. Proc. Am. Soc. Civil Eng. 89 (1963) 31–59.
[38] Y.S. Ho, G. McKay, Sorption of dye from aqueous solution by peat, Chem. Eng. J. 70 (1998) 115–124.
[39] F.I. Fu, Y. Xiong, B.P. Xie, R.M. Chen, Adsorption of Acid Red 73 on copper dithiocarbamate precipitate-type solid wastes, Chemosphere 66 (2007) 1–7.
[40] Q. Yue, J. Xie, B. Gao, Kinetics of adsorption of dyes by sludge activated carbon, Acta Sci. Circum. 27 (2007) 1431–1438.
[41] N. Thinakaran, P. Panneerselvamb, P. Baskaralingam, D. Elango, S. Sivanesan, Equilibrium and kinetic studies on the removal of Acid Red 114 from aqueous solutions using activated carbons prepared from seed shells, J. Hazard. Mater. 158 (2008) 142–150.
[42] F.C. Wu, R.L. Tseng, R.S. Juang, Enhanced abilities of highly swollen chitosan beads for color removal and tyrosinase immobilization, J. Hazard. Mater. 81 (2001) 167–177.
[43] Q.Y. Yue, J.K. Xie, B.Y. Gao, H. Yu, Kinetics of adsorption of dyes by sludge activated carbon, Acta Sci. Circum. 27 (2007) 1431–1438.